Peer-reviewed version available at Climate 2017, 5, 8; doi:10.3390/cli5010008

Article

Improving Hydro-Climatic Projections with Bias-Correction in Sahelian Niger Basin

Ganiyu Titilope Oyerinde [1,*], Fabien C.C. Hountondji [1,2], Agnide E. Lawin [3], Ayo J. Odofin [4], Abel Afouda [1] and Bernd Diekkrüger [5]

[1] Graduate Research Program (GRP) Climate Change and Water Resources, West African Science Service Center on Climate Change and Adapted Land Use (WASCAL), University of Abomey-Calavi, Abomey-Calavi, BP 2008, Benin; fabienho@yahoo.com (F.C.C.H.); aafouda@yahoo.fr (A.A.)
[2] Ecole Nationale Supérieure des Sciences et Techniques Agronomiques de Djougou, University of Parakou, Cadjéhoun 04, BP 123, Parakou, Benin
[3] Laboratory of Applied Hydrology, National Water Institute, University of Abomey-Calavi, Abomey-Calavi, BP 2008, Benin; ewaari@yahoo.fr
[4] Department of Soil Science and Land Management, Federal University of Technology, P.M.B 65, Gidan-Kwanu, Minna, Nigeria; odofinayo@yahoo.co.uk
[5] Department of Geography, University of Bonn, Meckenheimer Allee 166, 53115 Bonn, Germany; b.diekkrueger@uni-bonn.de
* Correspondence: ganiyuoyerinde@yahoo.com; Tel.: +234-703-683-5998

Abstract: Climate simulations in West Africa have been attributed with large uncertainties. Global climate projections are not consistent with changes in observations at the regional or local level of the Niger basin, making management of hydrological projects in the basin uncertain. This study evaluates the potential of using the quantile mapping bias correction to improve the Coupled Model Intercomparison Project (CMIP5) outputs for use in hydrology impact studies. Rainfall and temperature projections from 8 CMIP5 Global Climate Models (GCM) were bias corrected using the quantile mapping approach. Impacts of climate change was evaluated with bias corrected rainfall, temperature and potential evapotranspiration (PET). The IHACRES hydrological model was adapted to the Niger basin and used to simulate impacts of climate change on discharge under present and future conditions. Bias correction significantly improved the accuracy of rainfall and temperature simulations compared to observations. Nash coefficient (NSE) for monthly rainfall comparisons of 8 GCMs to the observed was improved by bias correction from 0.69 to 0.84. The standard deviations among the 8 GCM rainfall data were significantly reduced from 0.13 to 0.03. Increasing rainfall, temperature, PET and river discharge were projected for all GCMs used in this study under the RCP8.5 scenario. These results will help improving projections and contribute to the development of sustainable climate change adaptation strategies.

Keywords: climate change; evapotranspiration; IHACRES model; rainfall; runoff; quantile mapping

1. Introduction

Climate change impacts are expected to exacerbate poverty in most developing countries and create new poverty pockets in countries with increasing inequality in both developed and developing countries [1]. Water resources are fundamental for several sectors such as hydropower, crop production and fisheries in Africa [2]. Runoff evolutions in the region have been strongly affected by rainfall variations. Climate change has driven decreased discharge in West African rivers and increased drought in the Sahel since 1970 with partially wetter conditions experienced since 1990 [1,3,4]. Recently, reduction in rainfall of 10 to 30% on the Niger river has led to a deficit of 20 to 60% in river discharge [5]. Severe decrease of river flows in the basin was also observed mainly due to the 1970s' droughts [6].

Future climate simulations in the region have been a challenge for researchers using existing climate models [7]. Rapid forest disappearance or deterioration, especially due to population pressures and non-sustainable resource utilization [8], poses great challenge to land surface schemes of global climate model (GCM) and regional climate model (RCM). Consequently GCM projections in West Africa are accrued with different biases relative to regional observations and no coherent rainfall trend emerges from GCM products [9]. Vetter et al. [10] disclosed that scenarios from climate models are the largest uncertainty source, providing large discrepancies in precipitation, and therefore clear hydrological projections are difficult. Changes in hydrological regimes could become even more important in the future. In combination with the increasing demographic pressure and low adaptive capacity, these changes will have significant impacts on people and sectors that depend on water resources in West Africa [2]. Thus, there is a need to comprehend regional impacts of climate change on water resources.

Numerous studies [7,11–19] have assessed future trends of climate change in the region. Most of these studies either utilized the CMIP3 archive or worked on the large scale without giving finer basin scale information that are important for hydrological change evaluations. The studies showed that projections by GCMs are not consistent concerning the patterns of hydroclimatic changes and this makes management of hydrological projects difficult [20,21]. Recently, Biasutti [22] reported a more consistent trend in CMIP5 climate projections relative to CMIP3. Expectations of increasing rainfalls across the Sahel are also evident in CMIP5 climate projections [18,22]. However, with the recent attribution of CMIP5 datasets with regional biases and uncertainties [10,18,22,23], there is a need for improving the datasets in the assessments of impacts of climate change on water resources in the largest river basin in West Africa. Several ways have been applied to control biases in climate modeling. A comparative study among several bias correction approaches revealed that quantile mapping effectively corrected climate model biases and reduced systematic errors[24].

This study thereby enhanced datasets of 8 CMIP5 GCMs with bias correction and the improved datasets were used to evaluate future hydro-climatic conditions in the Sahelian Niger basin. The objectives of the study are to improve data projections, to assess projected trends of rainfall, temperature and PET and therefore climate change impacts on runoff in the Niger basin.

2. Materials and Methods

2.1 Study Area

The Niger River Basin covers an area of about 2.27 million km^2. The basin is drained by the third longest river in Africa [25] (Fig 1). The Niger basin covers different climatic zone with a very large percentage of it being in the Sahel. Upstream area of the evaluated hydrological station (Jidere bode) used in this study (Fig 1) covers about 1.61 million km^2 (about 70% of the basin). The hydrological station is located at the fringe of the Sahel in the Niger basin. Rainfall ranges from 250 to 750 mm/year in this region with a length of the rainy season varying from 3 to 7 months [20]. Two flooding regimes are prominent on the catchment. During May to October, flash floods from northern Benin and some parts of Niamey produce the white flood with a maximum flow of about 3500 m^3/s (based on observations from 1980 to 2010). The black flood comes from the river source region caused by high rainfall in November with a maximum flow of about 2000 m^3/s (based on observations from 1980 to 2010). Since 1990, more frequent extreme events in the two flooding regimes have led to increased floods in the Niger basin [26].

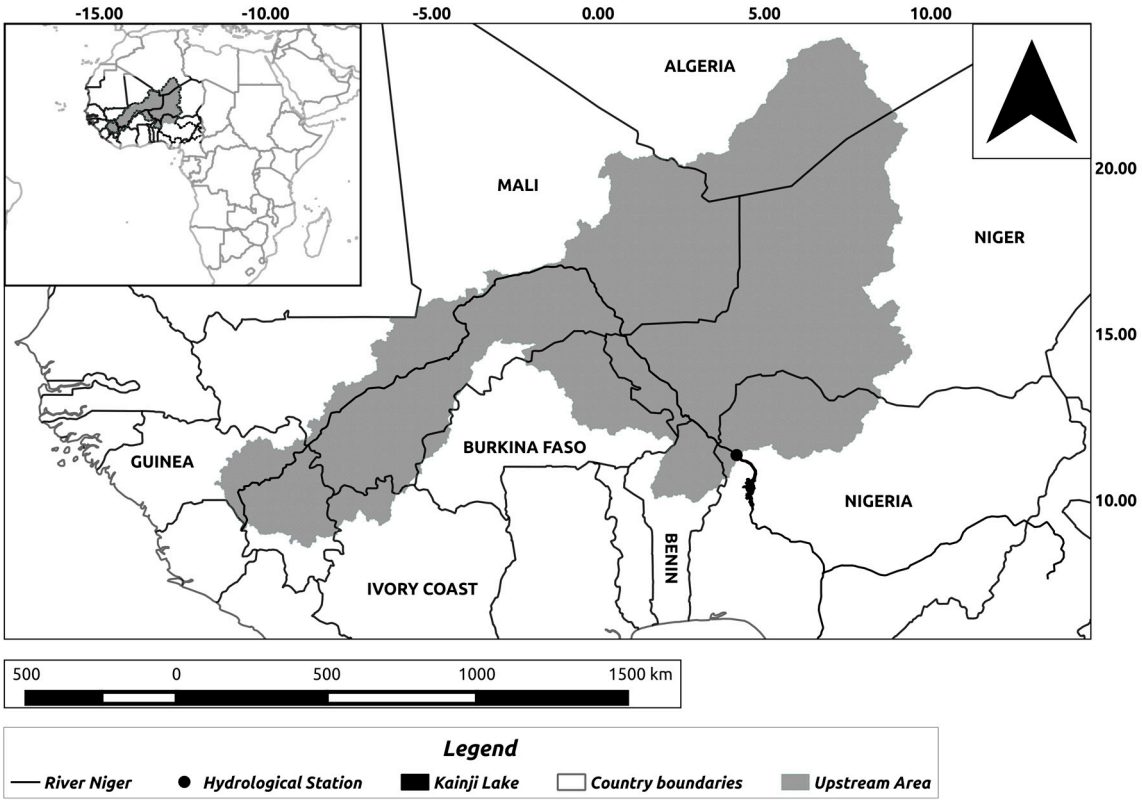

Figure 1. Upstream Niger basin area of Jidere bode hydrological station.

2.2 Hydrological Model

The hydrological model used in the present study, is a daily, lumped parameter, conceptual rainfall-runoff model which was implemented on the R based Hydromad [27,28]. It consists of three modules; the first was a non-linear IHACRES catchment wetness index (CWI) loss module [29]. CWI is chosen because it is the best configuration of IHACRES model in semi-arid regions [29,30]. The loss module which has five parameters converts rainfall to effective rainfall which is defined as the amount of rainfall that is not lost in the catchment [29,31,32]. The second was an ARMAX module with four parameters which was used for routing effective rainfall to stream flow [31,33]. The IHACRES model is a highly flexible model that readily allows coupling of new modules. In this study, a third module which fits the quantiles of simulated and observed discharge was introduced.

2.3 Data

The model needs daily rainfall, PET and river discharge as inputs. The Global Precipitation Climatology Project (GPCP) provided daily rainfall [34], daily temperature was obtained from the Modern Era Retrospective-Analysis for Research and Applications (MERRA) [35] and observed daily river discharge obtained from the Niger Basin Authority were used in the study. MERRA and GPCP were selected due to inadequate meteorological observation stations in the region [36]. The two datasets are available and commonly deployed in regional hydrological studies [37,38]. GPCP daily rainfall is known to have very low total bias to observed rainfall in the Sahel [38]. GPCP daily rainfall is available from 1997, MERRA temperature from 1979 and discharge data on the station highlighted in Fig 1 is available from 1980. Upstream area of the hydrological station (Fig 1) was delineated using a DEM provided by Hydrosheds (http://hydrosheds.cr.usgs.gov) using the Hortonian drainage networks analysis [39]. Rainfall and temperature distribution in West Africa have been attributed to the back and forth movement of the Inter Tropical Convergence Zone (ITCZ) [40]. The movement of the ITCZ follows the position of maximum surface heating associated with

meridional displacement of the overhead position of the sun. Due to the ITCZ, lower latitudes witness greater rainfall and cooler temperature while higher latitudes go through less rainfall and warmer temperatures. In order to account for the latitudinal ITCZ gradients, rainfall and temperature were computed using weighted average with latitudes. The latitudes were ranked and the ranks were used as weights for computing the averages. For computation of temperature, higher latitudes have higher ranks than lower latitudes while the reverse was applied for rainfall.

Catchment observed PET was computed from the extracted MERRA 2 meter daily air temperature using the Hamon model [41]. Future projections of rainfall and temperature data from 8 GCMs (Table 1) with two emission scenarios were used. They were dynamically downscaled to about 50 km resolution using the Sveriges Meteorologiska och Hydrologiska Institute - Rossby Centre Regional Atmospheric Model (SMHI-RCA) RCM within the Coordinated Regional Downscaling Experiment (CORDEX). The RCP4.5 and RCP8.5 scenarios were used in CORDEX-Africa CMIP5 simulations and they were evaluated in this study [42]. Future PET was computed from bias corrected temperature as described before. In line with the study of Su et al. [43], projected seasonal (meteorological) and monthly rainfall patterns in the "near future" (2010-2035) and "far future" (2036-2099) were compared to the historical period (1961-2005). Significance of changes in projected hydro-climatic variables was assessed with the student's t-test and the change point approach of Killick [44].

Table 1. List of CMIP5 GCMs considered in the study

Modeling Center (or Group)	**Country**	**Institute ID**	**Model Name**
Canadian Centre for Climate Modeling and Analysis	Canada	CCCMA	CanESM2
Centre National de Recherches Météorologiques / Centre Européen de Recherche et Formation Avancée en Calcul Scientifique	France	CNRM-CERFACS	CNRM-CM5
NOAA Geophysical Fluid Dynamics Laboratory	USA	NOAA GFDL	GFDL-ESM2M
Met Office Hadley Centre (additional HadGEM2-ES realizations contributed by Instituto Nacional de Pesquisas Espaciais)	UK	MOHC	HadGEM2-ES
Atmosphere and Ocean Research Institute (The University of Tokyo), National Institute for Environmental Studies, and Japan Agency for Marine-Earth Science and Technology	Japan	MIROC	MIROC5
Max-Planck-Institut für Meteorologie (Max Planck Institute for Meteorology)	Germany	MPI-M	MPI-ESM-LR
Norwegian Climate Centre	Norway	NCC	NorESM1-M
EC-EARTH consortium	Ireland	EC-EARTH	EC-EARTH

2.4 Bias Adjustment of GCM/RCMs and their Evaluation

Bias-correction removes errors from data from climate models in comparison with historical observations [45]. It relies on computation of differences between RCM/GCM and satellite-based estimates in regions with limited rain gauges [45]. In this study, the RCM/GCM datasets were bias corrected with daily MERRA and GPCP datasets from 1997 to 2010. The quantile mapping bias correction [19,24,46] was applied for improving the CMIP5 rainfall and temperature projections. The mapping was conducted separately for each month. The original daily RCM/GCM and bias corrected rainfall and temperature data were compared with the observed using six efficiency coefficients namely: Nash-Sutcliffe Efficiency ($\infty \leq NSE \leq 1$) [47], Index of Agreement ($0 \leq d \leq 1$) [48], Modified Index of Agreement ($0 \leq md \leq 1$) [48], Pearson Correlation coefficient ($-1 \leq r \leq 1$) [48], Coefficient of Determination ($0 \leq R^2 \leq 1$) [48] and Kling-Gupta efficiency ($0 \leq KGE \leq 1$) [45]. The levels of significance of the improvements were measured with t-test.

2.5 Hydrological model evaluation

Hydrological model evaluation was conducted for fourteen years (1997-2010) using GPCP daily rainfall, PET and observed river discharge. Calibration of the hydrological model was done for the period 1997-2003 while validation for the period 2004-2010. The choice of the calibration time span was based on data availability. Shin et al. [49] reported five years as the minimum length of daily records required to attain stable IHACRES parameters. The model was automatically calibrated for the stipulated periods with the optimization of the Nash efficiency. During future projections, the GPCP daily rainfall, PET (computed from observed temperature) and observed river discharges were used to set the model parameters through an independent fourteen years calibration (1997-2010). The pre-calibrated hydrological model was used to predict daily runoff with bias corrected rainfall and PET (computed from bias corrected temperature projections) datasets from 8 GCMs under two emission scenarios from the CORDEX regional downscaling experiments.

3. Results

3.1 CMIP5 model improvements with Bias Correction

Comparison of the models (8 GCMs) and bias corrected simulations to the GPCP and MERRA observed rainfall and temperature are presented in Fig 2. All evaluated GCMs underestimated daily climatological (daily mean from 1997-2010) and monthly catchment rainfall and temperature and this was adequately corrected by bias correction (Fig 2). Mean and standard deviation of correlation efficiency coefficients to observed among the 8 GCMs (Table 2 and 3) were significantly ($p < 0.05$) improved by bias correction during seasonal, monthly and daily climatological comparisons (Table 2). Individual GCM monthly correlation efficiency coefficients (Table 3) before bias correction revealed that CNRM-CM5 (*NSE* = 0.81) had the highest correlation with observed while NorESM1-M (*NSE* = 0.46) had the lowest. Temperature indicated that MIROC5 (*NSE* = 0.86) best predicts the catchment temperature while EC-EARTH (*NSE* = 0.45) had a poor prediction. Bias correction improved the correlation coefficients of all the 8 GCMs with rainfall *NSE* being about 0.80 and temperature *NSE* was above 0.90 for all the GCMs (Table 3).

Preprints (www.preprints.org) | NOT PEER-REVIEWED | Posted: 7 December 2016 doi:10.20944/preprints201612.0037.v1

Peer-reviewed version available at Climate 2017, 5, 8; doi:10.3390/cli5010008

Table 2. Means and standard deviations of efficiency coefficients (8 GCMs) compared to observations before and after bias correction at monthly, seasonal (meteorological) and climatological time frames

Efficiency Coefficients	Rainfall				Temperature			
	Before		Bias Corrected		Before		Bias Corrected	
	Mean	Std	Mean	Std	Mean	Std	Mean	Std
Monthly								
NSE	0.69	0.13	0.84	0.03	0.67	0.16	0.96	0.01
D	0.91	0.05	0.96	0.01	0.92	0.04	0.99	< 0.01
Md	0.78	0.05	0.85	0.01	0.71	0.08	0.91	0.01
R	0.86	0.06	0.93	0.01	0.97	0.00	0.98	< 0.01
R^2	0.74	0.10	0.86	0.02	0.95	0.01	0.96	0.01
KGE	0.75	0.14	0.90	0.02	0.87	0.03	0.98	< 0.01
Seasonal (meteorological season)								
NSE	0.76	0.14	0.92	0.02	0.64	0.19	0.98	0.01
D	0.93	0.05	0.98	0.01	0.92	0.04	0.99	< 0.01
Md	0.78	0.07	0.88	0.01	0.67	0.08	0.92	0.01
R	0.91	0.05	0.96	0.01	0.98	0.01	0.99	< 0.01
R^2	0.83	0.09	0.92	0.02	0.97	0.00	0.98	0.01
KGE	0.76	0.14	0.94	0.02	0.87	0.03	0.99	0.01
Climatological (daily mean from 1997-2010)								
NSE	0.74	0.15	0.90	0.02	0.71	0.15	1.00	0.01
D	0.92	0.05	0.98	0.00	0.93	0.04	1.00	< 0.01
Md	0.80	0.06	0.89	0.01	0.71	0.08	0.97	< 0.01
R	0.89	0.06	0.96	0.01	0.99	0.00	1.00	< 0.01
R^2	0.79	0.11	0.91	0.01	0.98	0.01	1.00	0.01
KGE	0.76	0.15	0.94	0.01	0.87	0.03	1.00	< 0.01

Table 3. Monthly efficiency coefficients of 8 GCMs compared to observations before and after bias correction.

GCMs	Before						Bias corrected					
	NSE	d	Md	r	R^2	KGE	NSE	d	md	r	R^2	KGE
	Rainfall											
GFDL-ESM2M	0.74	0.93	0.8	0.87	0.76	0.85	0.79	0.95	0.83	0.91	0.82	0.87
NorESM1-M	0.46	0.84	0.71	0.73	0.53	0.69	0.82	0.96	0.85	0.92	0.84	0.9
MPI-ESM-LR	0.8	0.95	0.82	0.9	0.81	0.87	0.87	0.97	0.86	0.94	0.88	0.92
HadGEM2-ES	0.78	0.94	0.81	0.89	0.79	0.87	0.85	0.96	0.84	0.93	0.86	0.91
MIROC5	0.76	0.93	0.8	0.87	0.76	0.83	0.85	0.96	0.85	0.93	0.86	0.91
EC-EARTH	0.64	0.89	0.75	0.82	0.67	0.72	0.85	0.96	0.86	0.93	0.87	0.91
CNRM-CM5	0.81	0.95	0.82	0.93	0.86	0.76	0.84	0.96	0.85	0.93	0.86	0.9
CanESM2	0.52	0.84	0.69	0.88	0.77	0.44	0.88	0.97	0.87	0.94	0.89	0.91
	Temperature											
GFDL-ESM2M	0.54	0.89	0.64	0.97	0.94	0.87	0.95	0.99	0.9	0.97	0.95	0.97
NorESM1-M	0.73	0.93	0.72	0.97	0.94	0.88	0.96	0.99	0.92	0.98	0.96	0.98

MPI-ESM-LR	0.75	0.94	0.73	0.98	0.96	0.9	0.97	0.99	0.92	0.98	0.97	0.98
HadGEM2-ES	0.75	0.94	0.73	0.97	0.94	0.89	0.96	0.99	0.91	0.98	0.96	0.98
MIROC5	0.86	0.96	0.8	0.97	0.94	0.83	0.96	0.99	0.92	0.98	0.96	0.98
EC-EARTH	0.45	0.87	0.6	0.97	0.95	0.82	0.96	0.99	0.91	0.98	0.96	0.98
CNRM-CM5	0.48	0.88	0.62	0.97	0.94	0.86	0.96	0.99	0.92	0.98	0.96	0.98
CanESM2	0.81	0.96	0.8	0.98	0.96	0.89	0.96	0.99	0.91	0.98	0.96	0.98

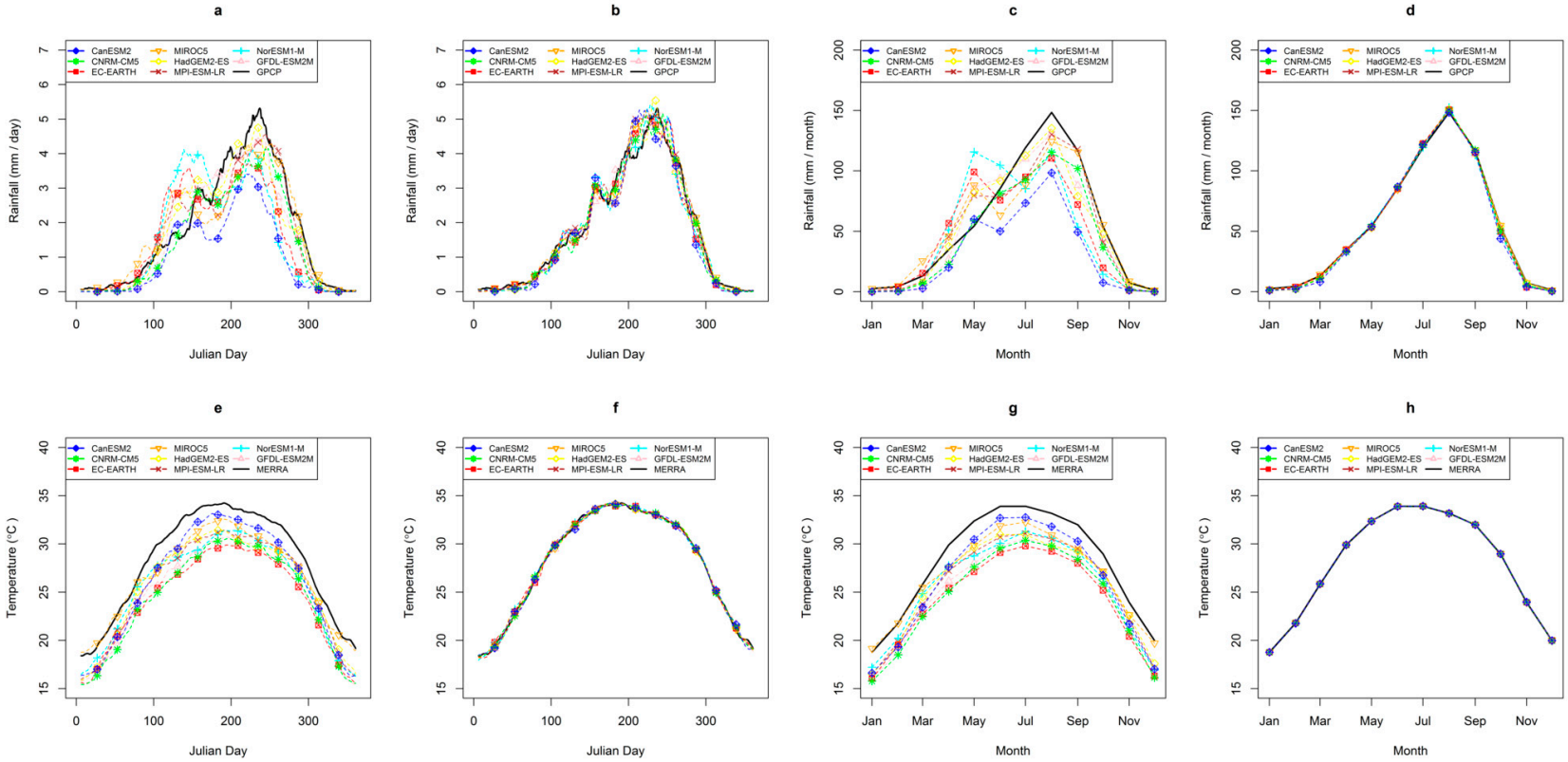

Figure 2. Comparison of CMIP5 rainfall and temperature simulations with GPCP and MERRA before and after bias correction for the evaluation period (1997-2010). (a) climatological (daily mean from 1997-2010) rainfall before bias correction (b) climatological rainfall after bias correction (c) monthly rainfall before bias correction (d) monthly rainfall after bias correction (e) climatological temperature before bias correction (f) climatological temperature after bias correction (g) monthly temperature before bias correction (h) monthly temperature after bias correction

Preprints (www.preprints.org) | NOT PEER-REVIEWED | Posted: 7 December 2016 doi:10.20944/preprints201612.0037.v1

Peer-reviewed version available at Climate 2017, 5, 8; doi:10.3390/cli5010008

During hydrological model calibration and validation (Fig 3), high correlation efficiency coefficients were observed between simulated and observed runoff. Efficiency coefficients of 0.92 (*NSE*), 0.98 (*d*), 0.89 (*md*), 0.96 (*r*), 0.92 (R^2) and 0.96 (*KGE*) were recorded for model calibration, while 0.80 (*NSE*), 0.95 (*d*), 0.82 (*md*), 0.91 (*r*), 0.83 (R^2) and 0.88 (*KGE*) were recorded for model validation. This implies that the model was able to adequately simulate river discharge in the Niger basin and could be used in projecting runoff trends.

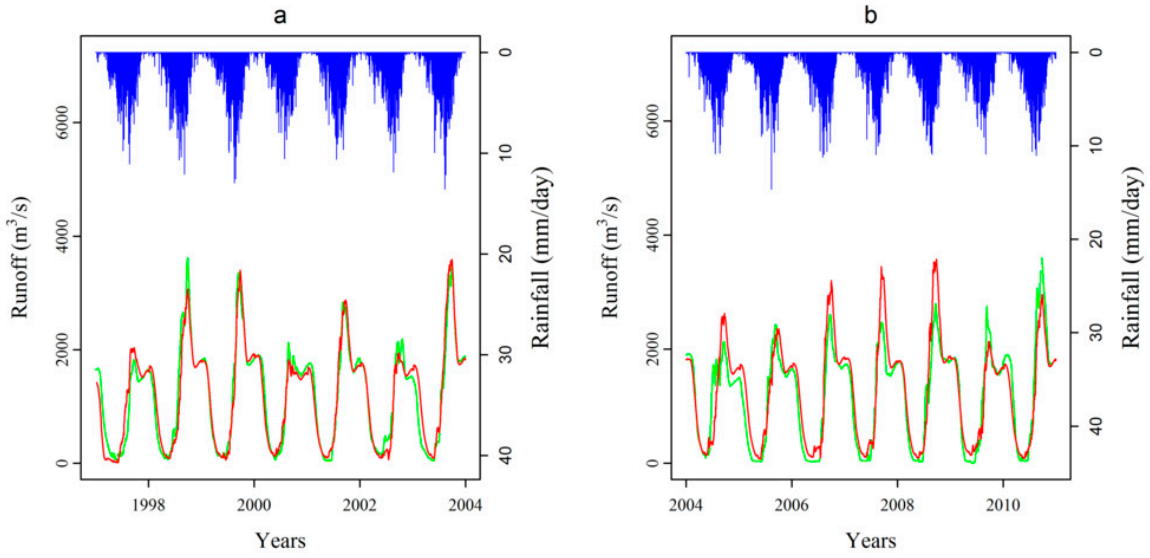

Figure 3. Calibration (a) and validation (b) of the hydrological model with observed data in the Niger Basin; inverted bars represent GPCP rainfall while broken and solid lines are observed and simulated runoff respectively

3.2 Hydroclimatic Projections

Annual and monthly projected rainfall, temperature, PET and runoff ensemble medians from 8 GCMs are displayed in Fig 4 and 5 respectively.

3.3 Rainfall

Annual rainfall will go through a highly significant ($p < 0.01$) regime shift at 2050 with about 80 mm (RCP8.5) increase relative to the historical average (Fig 4a). Under RCP4.5, about 40 mm highly significant ($p < 0.01$) upward shift at 2019 will be experienced. Monthly near and far future rainfall trends are presented in Fig 5. Higher changes were observed for August and September under the two scenarios for both terms. Under RCP4.5 scenario, the near future (Fig 5a) will be ascribed with significant ($p < 0.05$) rainfall decrease at January and March. Significant increase ($p < 0.05$) will be witnessed at July while August and September will experience a highly significant increase ($p < 0.01$). At the far future (Fig 5b), highly significant decrease ($p < 0.01$) in rainfall will be prominent at January while highly significant increases ($p < 0.01$) will be witnessed at July, August and September. RCP8.5 near future (Fig 5a) will be characterized by no significant decrease in rainfall, highly significant ($p < 0.01$) increases will be witnessed at September while significant increase ($p < 0.05$) will be prominent in June, July and August. At the far future (Fig 5b), RCP8.5 will be characterized by highly significant ($p < 0.01$) decrease in rainfall at January and December (significant at $p < 0.05$) while highly significant increases will be witnessed at July, August and September and significant increases ($p < 0.05$) are expected at May, June and October .

Preprints (www.preprints.org) | NOT PEER-REVIEWED | Posted: 7 December 2016 doi:10.20944/preprints201612.0037.v1

Peer-reviewed version available at Climate 2017, 5, 8; doi:10.3390/cli5010008

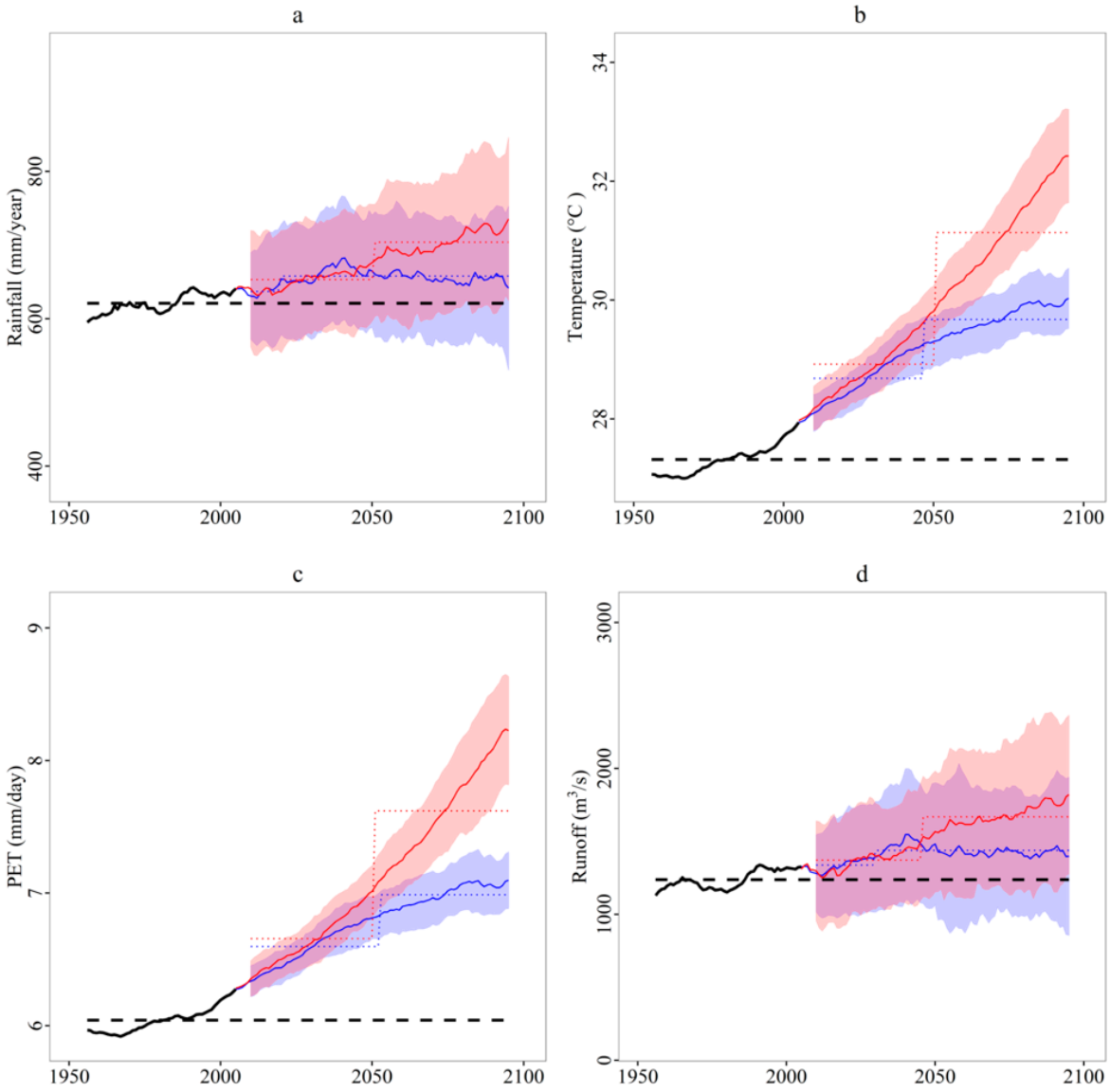

Figure 4. Projected annual climate and runoff trends from eight GCMs in the Niger Basin. (a) rainfall (b) temperature (c) PET (d) runoff: thick black line represents ensemble median historical trend (1961-2005), triangular lines represent ensemble median RCP8.5, cyclic lines represent ensemble median RCP4.5; standard deviations across the GCMs are shown in surrounding bounds. Dotted lines show significant ($p < 0.01$) regime shifts and dashed black lines is the historical mean

3.4 Temperature

Projected annual, monthly and seasonal temperature will experience highly significant ($p < 0.01$) increases under the two scenarios and terms. With respect to the historical mean - at mid century – annual average temperature will go through about 3.5 °C upward regime shift under RCP8.5 compared with about 2 °C rise under RCP4.5 (Fig 4b). About 1-2°C increase in temperature will be experienced across the months in the near future (Fig 5c) while the far future (Fig 5d) will be attributed with about 2-4°C increase in temperature under the two scenarios.

3.5 PET

In the RCP8.5 scenario, there will be a significant increase of more than 1.5 mm/d ($p < 0.01$) in PET with respect to historical data while under RCP4.5, the increase ($p < 0.01$) will be about 1 mm/day at mid-century (Fig 4c). Monthly PET will experience about 0.2-0.7 mm/day ($p < 0.01$)

increase all through the months in the near future (Fig 5e) while in the far future (Fig 5f) about 0.5-2.0 mm/day ($p < 0.01$) increase is expected under the two scenarios.

3.6 Runoff

In the RCP8.5 scenario, there will be an upward (+400 m^3/s relative to historical period) highly significant ($p < 0.01$) shift in the annual mean runoff at mid-century while about 200 m^3/s increase ($p < 0.01$) will be attributed to RCP4.5 at 2031 (Fig 4d). Monthly near future showcased increases of varying magnitude throughout the months for both scenarios and time slices (Fig 5). Under RCP4.5 scenario, monthly highly significant ($p < 0.01$) increases relative to historical mean are projected at the near future (Fig 5g) at January, February, March , April, September, October, November and December while significant increases at $p < 0.05$ will be attributed with May and August. At the far future (Fig 5h), highly significant ($p < 0.01$) increase in runoff will be observed in January, February, March, April, May, August, September, October, November and December. RCP8.5 near future (Fig 5g) increases ($p < 0.01$) are projected in the months of January, February, March, April, September, October, November and December while increases at July and August will be significant at $p < 0.05$. At the far future (Fig 5f) all the months will be attributed with significant ($p < 0.01$) runoff increases. In the Near Future (Table 4), all models and the ensemble predict increases in the two scenarios except EC-EARTH and MPI-ESM-LR (RCP 45) where decreases in runoff are expected. Far Future runoff will experience increases with agreements of all models and ensemble under both scenario.

Table 4. Percentage runoff trends at the near future (NF, 2010-2035) and far future (FF, 2036-2100) relative to the historical (1961-2000)

MODELS	Runoff (%)			
	NF		FF	
	RCP 45	RCP 85	RCP 45	RCP 85
CanESM2	13.53	11.28	23.85	41.50
CNRM-CM5	2.31	4.66	12.91	37.20
EC-EARTH	-1.91	-4.79	6.20	15.37
MIROC5	29.31	24.68	43.88	81.99
HadGEM2-ES	11.63	19.74	15.13	28.68
MPI-ESM-LR	-0.93	10.46	0.09	11.65
NorESM1-M	12.88	18.18	22.82	38.91
GFDL-ESM2M	6.73	16.27	24.90	31.34
ENSMED	8.78	11.95	18.45	34.91

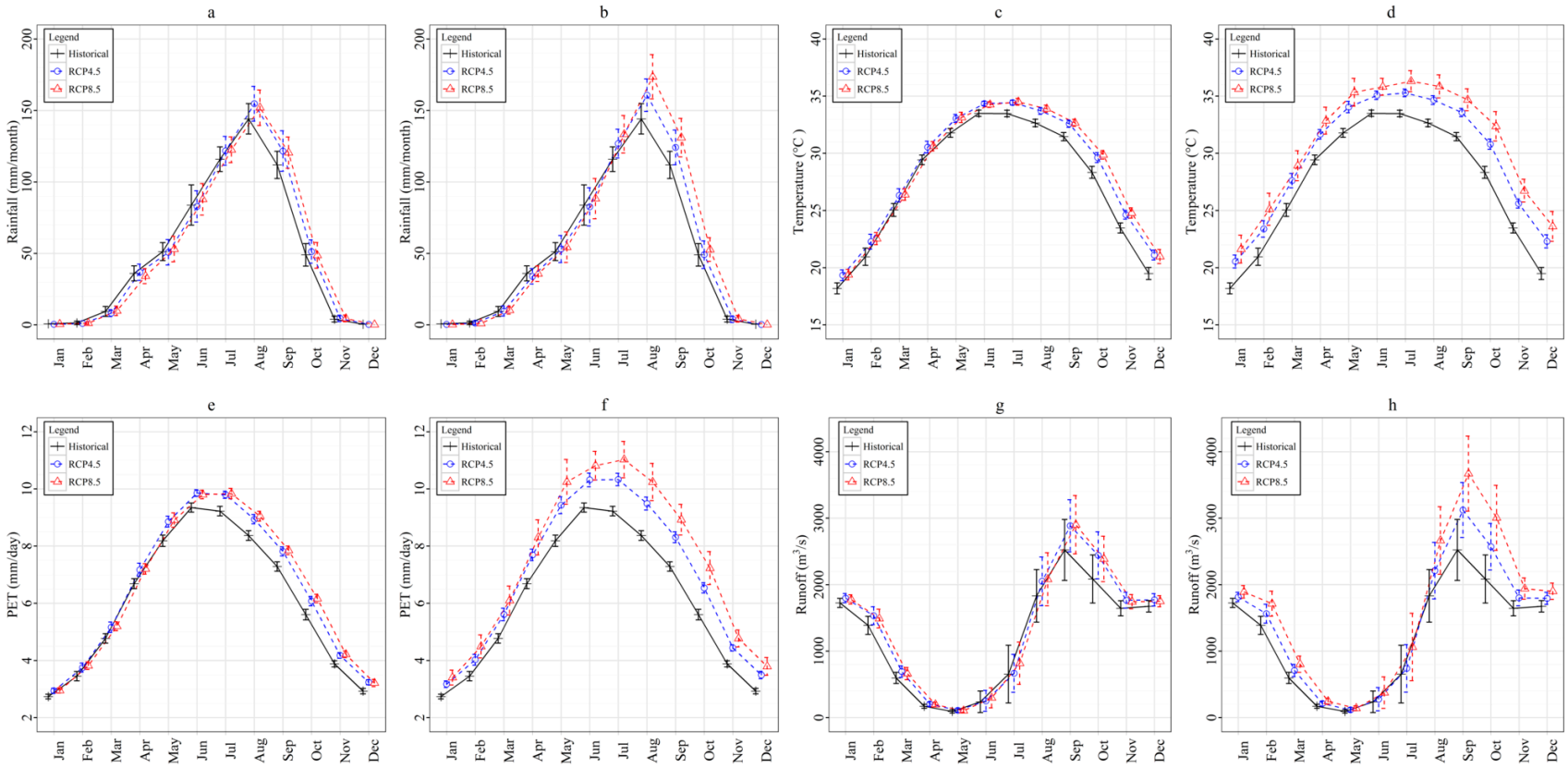

Figure 5. Ensemble median projected monthly hydro-climatic projections from eight GCMs in the near (2010-2035) and far (2036-2099) future. (a) near future rainfall (b) far future rainfall (c) near future temperature (d) far future temperature (e) near future PET (f) far future PET (g) near future runoff (h) far future runoff: points indicates the within month means while error bars gives the within month standard deviations of the ensemble median.

4. Discussion

The reduction of deviations among the 8 evaluated GCMs (Fig 2) by quantile mapping indicated the appropriateness of the method for the Niger basin. It was able to improve the correlations between observed and simulated rainfall and temperature. Most climate models, for example, tend to overestimate the amount of "drizzle" [50,51] and consequently generate biased data compared to observations [52]. CMIP5 models have also been attributed with such biases in West Africa [18,22]. The improvement of simulations with bias correction applied to the catchment suggests the appropriateness of the method. The improved hydrological model implemented here is a lumped parameter, conceptual rainfall-runoff model [29,32]. Hydrological model efficiency was evaluated by comparing simulated and observed runoff. Downscaled re-analysis was earlier shown to cause ineffective modeling for hydrological models [38]. Results here indicate that the adapted model appropriately simulates river discharge using re-analysis data and therefore gives possibility for its application to poorly/ungauged basin.

The simulations predict an increase in rainfall in Sahelian parts of the Niger basin in agreement with previous studies in future. Biasutti [22] showed that the majority of the CMIP5 models project a wetter Sahel in the 21st century. Sylla et al. [16] also reported a more pronounced increase of the intensity of very wet rainfall events in the Sahel towards the end of the century. Decrease in rainfall in the months at the beginning of the rainy season will hamper water availability in these difficult periods. Apata et al. [53] showed that an increase of the length of the dry season have aggravated the challenges of drying-out of streams and small rivers that usually flows year round. It has also led to the seasonal shifting of the "Mango rains" and of the fruiting period [53]. These climate change issues will persist and aggravate as indicated in both scenarios. Projected high increases in rainfall in the wet months will lead to concurrent increases in runoff especially in the two flooding seasons (white flood and black flood). Similar patterns of runoff increase in the Niger basin due to rainfall increase was reported by Roudier et al [2]. This will aggravate the current problematic flooding in the region [26,54] which was already attributed to increasing rainfall trends and reduced infiltration due to replacement of natural (permeable) surfaces by man-made (impermeable) surfaces [8].

5. Conclusions

Changes in hydrological regimes could become more important in the future. In combination with the increasing demographic pressure and low adaptive capacity, these changes will have significant impacts on people and sectors that depend on the availability of water in West Africa [2]. High discrepancies in rainfall-runoff projections have hampered sustainable management of hydrological projects in the Niger basin [20]. This paper showcased that the recent CMIP5 archive and concurrent bias improvements have a great potential for reducing these discrepancies. The bias corrected CMIP5 projected rainfall-runoff patterns presented in this study showed higher confidence than previous simulations in the Niger basin; and appears to be an important tool for hydroclimatic predictions. The persisting and aggravating hydroclimatic trends disclosed under the two scenarios suggest investing more efforts towards the development of adaptation techniques, particularly in the water supply and conservation, agriculture and energy sectors. Further research will consider applying this modeling framework to various basin scales and evaluate impacts of climate change on water-related sectors, particularly water supply, agriculture and energy, which are important economic sectors in the basin, for improved adaptation strategies.

Acknowledgments: This study was funded by the German Ministry of Education and Research (BMBF) through the Center for Development Research and WASCAL-GRP CC&WR at the University of Abomey Calavi. ESGF grid (http://esg-dn1.nsc.liu.se/esgf-web-fe/) which provides CORDEX-Africa data is appreciated. The Niger Basin Authority is appreciated for providing the river discharge data.

Author Contributions: All figures and tables were done by Ganiyu Titilope Oyerinde, Fabien C.C. Hountondji and Bernd Diekkrüger. Manuscript writing was made by Ganiyu Titilope Oyerinde, Fabien C.C. Hountondji and Bernd Diekkrüger. The PhD thesis where the manuscript was derived from was supervised and examined by Fabien C.C. Hountondji, Ayo J. Odofin, Abel Afouda and Agnide E. Lawin.

Conflicts of Interest: The authors declare no conflict of interest.

References

1. IPCC Summary for policymakers. In *Climate Change 2014:Impacts, Adaptation, and Vulnerability. Part A: Global and Sectoral Aspects. Contribution of Working Group II to the Fifth Assessment Report of the Intergovernmental Panel on Climate Change*; Field, C. B.; Barros, V. R.; Dokken, D. J.; Mach, K. J.; Mastrandrea, M. D.; Bilir, T. E.; Chatterjee, M.; Ebi, K. L.; Estrada, Y. O.; Genova, R. C.; Girma, B.; Kissel, E. S.; Levy, A. N.; MacCracken, S.; Mastrandrea, P. R.; White, L. L., Eds.; Cambridge University Press, Cambridge, United Kingdom and New York, NY, USA, 2014; pp. 1–32.

2. Roudier, P.; Ducharne, A.; Feyen, L. Climate change impacts on river discharge in West Africa: a review. *Hydrol. Earth Syst. Sci. Discuss.* **2014**, *11*, 2483–2514.

3. Lebel, T.; Ali, A. Recent trends in the Central and Western Sahel rainfall regime (1990–2007). *J. Hydrol.* **2009**, *375*, 52–64.

4. Amogu, O.; Descroix, L.; Yéro, K. S.; Le Breton, E.; Mamadou, I.; Ali, A.; Vischel, T.; Bader, J.-C.; Moussa, I. B.; Gautier, E.; Boubkraoui, S.; Belleudy, P. Increasing River Flows in the Sahel? *Water* **2010**, *2*, 170–199.

5. Novotny, E. V.; Stefan, H. G. Stream flow in Minnesota: Indicator of climate change. *J. Hydrol.* **2007**, *334*, 319–333.

6. Lebel, T.; Diedhiou, A.; Henri, L. Seasonal cycle and interannual variability of the Sahelian rainfall at hydrological scales. *J. Geophys. Res.* **2003**, *108*, 1–11.

7. Laprise, R.; Hernández-Díaz, L.; Tete, K.; Sushama, L.; Šeparović, L.; Martynov, A.; Winger, K.; Valin, M. Climate projections over CORDEX Africa domain using the fifth-generation Canadian Regional Climate Model (CRCM5). *Clim. Dyn.* **2013**, *41*, 3219–3246.

8. Chineke, T.; Idinoba, M. Seasonal evapotranspiration signatures under a changing landscape and ecosystem management in Nigeria: Implications for agriculture and food security. *Am. J. Sci. Ind. Res.* **2011**, *2*, 191–204.

9. Druyan, L. M. Studies of 21st-century precipitation trends over West Africa. *Int. J. Climatol.* **2011**, *31*, 1415–1424.

10. Vetter, T.; Huang, S.; Aich, V.; Yang, T.; Wang, X.; Krysanova, V.; Hattermann, F. Multi-model climate impact assessment and intercomparison for three large-scale river. *Earth Syst. Dyn.* **2015**, *6*, 17–43.

11. Diallo, I.; Sylla, M. B.; Giorgi, F.; Gaye, A. T.; Camara, M. Multimodel GCM-RCM Ensemble-Based Projections of Temperature and Precipitation over West Africa for the Early 21st Century. *Int. J. Geophys.* **2012**, *2012*, 1–19.

12. Mertz, O.; D'haen, S.; Maiga, A.; Moussa, I. B.; Barbier, B.; Diouf, A.; Diallo, D.; Da, E. D.; Dabi, D. Climate variability and environmental stress in the Sudan-Sahel zone of West Africa. *Ambio* **2012**, *41*, 380–92.

13. Mariotti, L.; Coppola, E.; Sylla, M. B.; Giorgi, F.; Piani, C. Regional climate model simulation of projected 21st century climate change over an all-Africa domain: Comparison analysis of nested and driving model results. *J. Geophys. Res.* **2011**, *116*, D15111.

14. Oguntunde, P. G.; Abiodun, B. J. The impact of climate change on the Niger River Basin hydroclimatology , West Africa. *Clim. Dyn.* **2013**, *40*, 81–94.

15. Panitz, H.-J.; Dosio, A.; Büchner, M.; Lüthi, D.; Keuler, K. COSMO-CLM (CCLM) climate simulations over CORDEX-Africa domain: analysis of the ERA-Interim driven simulations at 0.44° and 0.22° resolution. *Clim. Dyn.* **2013**, *42*, 3015–30.

16. Sylla, M. B.; Giorgi, F.; Pal, J. S.; Gibba, P.; Kebe, I.; Nikiema, M. Projected Changes in the Annual Cycle of High Intensity Precipitation Events over West Africa for the Late 21st Century. *J. Clim.* **2015**, 150522112645005.

17. Sylla, M. B.; Gaye, A. T.; Jenkins, G. S.; Pal, J. S.; Giorgi, F. Consistency of projected drought over the Sahel

with changes in the monsoon circulation and extremes in a regional climate model projections. *J. Geophys. Res.* **2010**, *115*, D16108.

18. Klutse, N. A. B.; Sylla, M. B.; Diallo, I.; Sarr, A.; Dosio, A.; Diedhiou, A.; Kamga, A.; Lamptey, B.; Ali, A.; Gbobaniyi, E. O.; Owusu, K.; Lennard, C.; Hewitson, B.; Nikulin, G.; Panitz, H.-J.; Büchner, M. Daily characteristics of West African summer monsoon precipitation in CORDEX simulations. *Theor. Appl. Climatol.* **2015**, 1–17.

19. Oyerinde, G. T.; Wisser, D.; Hountondji, F. C. C.; Odofin, A. J.; Lawin, A. E.; Afouda, A.; Diekkrüger, B. Quantifying Uncertainties in Modeling Climate Change Impacts on Hydropower Production. *Climate* **2016**, *4*, 1–15.

20. KfW Adaptation to climate change in the upper and middle Niger River Basin. River Basin snapshot, draft for discussion, Entwicklungsbank, May 2010, p 41. **2010**.

21. Ghile, Y. B.; Taner, M. Ü.; Brown, C.; Grijsen, J. G. Bottom-up climate risk assessment of infrastructure investment in the Niger River Basin. *Clim. Change* **2014**, *122*, 97–110.

22. Biasutti, M. Forced Sahel rainfall trends in the CMIP5 archive. *J. Geophys. Res. Atmos.* **2013**, *118*, 1613–1623.

23. Gbobaniyi, E.; Sarr, A.; Sylla, M. B.; Diallo, I.; Lennard, C.; Dosio, A.; Dhiédiou, A.; Kamga, A.; Klutse, N. A. B.; Hewitson, B.; Nikulin, G.; Lamptey, B. Climatology, annual cycle and interannual variability of precipitation and temperature in CORDEX simulations over West Africa. *Int. J. Climatol.* **2014**, *34*, 2241–2257.

24. Gudmundsson, L.; Bremnes, J. B.; Haugen, J. E.; Engen-Skaugen, T. Technical Note: Downscaling RCM precipitation to the station scale using statistical transformations - A comparison of methods. *Hydrol. Earth Syst. Sci.* **2012**, *16*, 3383–3390.

25. Ogilvie, A.; Mahéé, G.; Ward, J.; Serpantiéé, G.; Lemoalle, J.; Morand, P.; Barbier, B.; Kaczan, D.; Lukasiewicz, A.; Paturel, J.; Liéénou, G.; Clanet, J. C. Water, agriculture and poverty in the Niger River basin. *Water Int.* **2010**, *35*, 594–622.

26. Oyerinde, G. T.; Hountondji, F. C. C.; Wisser, D.; Diekkrüger, B.; Lawin, A. E.; Odofin, A. J.; Afouda, A. Hydro-climatic changes in the Niger basin and consistency of local perceptions. *Reg. Environ. Chang.* **2015**, *15*, 1627–1637.

27. Andrews, F. T.; Croke, B. F. W.; Jakeman, A. J. An open software environment for hydrological model assessment and development. *Environ. Model. Softw.* **2011**, *26*, 1171–1185.

28. R Development Core Team R: A language and environment for statistical computing http://www.r-project.org. (accessed Aug 13, 2015).

29. Ye, W.; Bates, B. C.; Viney, N. R.; Sivapalan, M. Performance of conceptual rainfall-runoff models in low-yielding ephemeral catchments. *Water Resour. Res.* **1997**, *33*, 153–166.

30. Croke, B.; Jakeman, A. Use of the IHACRES rainfall-runoff model in arid and semi arid regions. In *Hydrological modelling in arid and semi-arid areas*; Wheater, H.; Sorooshian, S.; Sharma, K. D., Eds.; Cambridge University Press, 2008; pp. 41–48.

31. Andrews, F. ARMAX Transfer Function models. http://hydromad.catchment.org/man/armax.html (accessed Mar 30, 2016).

32. Jakeman, A. J.; Littlewood, I. G.; Whitehead, P. G. Computation of the instantaneous unit hydrograph and identifiable component flows with application to two small upland catchments. *J. Hydrol.* **1990**, *117*, 275–300.

33. Dutta, D.; Welsh, W.; Vaze, J.; Kim, S.; Nicholls, D. Improvement in short-term streamflow forecasting using an integrated modelling framework. *19th Int. Congr. Model. Simulation, Perth, Aust. 12–16 December* **2011**.

34. Huffman, G. J.; Adler, R. F.; Arkin, P.; Chang, A.; Ferraro, R.; Gruber, A.; Janowiak, J.; Mcnab, A.; Rudolf, B.; Schneider, U. The Global Precipitation Climatology Project (GPCP) Combined Precipitation Dataset. *Bull. Am. Meteorol. Soc.* **1997**, *78*, 5–20.

35. Rienecker, M. M.; Suarez, M. J.; Gelaro, R.; Todling, R.; Bacmeister, J.; Liu, E.; Bosilovich, M. G.; Schubert, S. D.; Takacs, L.; Kim, G. K.; Bloom, S.; Chen, J.; Collins, D.; Conaty, A.; Da Silva, A.; Gu, W.; Joiner, J.; Koster, R. D.; Lucchesi, R.; Molod, A.; Owens, T.; Pawson, S.; Pegion, P.; Redder, C. R.; Reichle, R.; Robertson, F. R.; Ruddick, A. G.; Sienkiewicz, M.; Woollen, J. MERRA: NASA's modern-era retrospective analysis for research and applications. *J. Clim.* **2011**, *24*, 3624–3648.

36. Ali, A.; Lebel, T. The Sahelian standardized rainfall index revisited. *Int. J. Climatol.* **2009**, *29*, 1705–1714.

37. Jobard, I.; Chopin, F.; Berges, J. C.; Roca, R. An intercomparison of 10-day satellite precipitation products during West African monsoon. *Int. J. Remote Sens.* 2011, *32*, 2353–2376.

38. Gosset, M.; Viarre, J. Evaluation of several rainfall products used for hydrological applications over West Africa using two high-resolution gauge networks. *Q. Jounal R. Meteorol. Soc.* **2013**, *139*, 923–940.

39. Jasiewicz, J.; Metz, M. A new GRASS GIS toolkit for Hortonian analysis of drainage networks. *Comput. Geosci.* **2011**, *37*, 1162–1173.

40. Lucio, P.; Molion, L.; Valadão, C.; Conde, F.; Ramos, A.; MLD, M. Dynamical outlines of the rainfall variability and the ITCZ role over the West Sahel. *Atmos. Clim. Sci.* **2012**, *2*, 337–350.

41. Oudin, L.; Hervieu, F.; Michel, C.; Perrin, C.; Andréassian, V.; Anctil, F.; Loumagne, C. Which potential evapotranspiration input for a lumped rainfall–runoff model? *J. Hydrol.* **2005**, *303*, 290–306.

42. Giorgi, F.; Jones, C.; Asrar, G. R. Addressing climate information needs at the regional level: the CORDEX framework. *WMO Bull.* **2009**, *58*, 175–183.

43. Su, F.; Duan, X.; Chen, D.; Hao, Z.; Cuo, L. Evaluation of the Global Climate Models in the CMIP5 over the Tibetan Plateau. *J. Clim.* **2013**, *26*, 3187–3208.

44. Killick, R. changepoint : An R Package for Changepoint Analysis. *J. Stat. Softw.* **2014**, *58*, 1–19.

45. Kling, H.; Fuchs, M.; Paulin, M. Runoff conditions in the upper Danube basin under an ensemble of climate change scenarios. *J. Hydrol.* **2012**, *424-425*, 264–277.

46. Ravazzani, G.; Dalla Valle, F.; Gaudard, L.; Mendlik, T.; Gobiet, A.; Mancini, M. Assessing Climate Impacts on Hydropower Production: The Case of the Toce River Basin. *Climate* **2016**, *4*, 16.

47. Nash, J. E.; Sutcliffe, J. V. River flow forecasting through conceptual models part I — A discussion of principles. *J. Hydrol.* 1970, *10*, 282–290.

48. Legates, D. R.; McCabe, G. J. Evaluating the use of "goodness-of-fit" measures in hydrologic and hydroclimatic model validation. *Water Resour. Res.* **1999**, *35*, 233–241.

49. Shin, M.; Guillaume, J.; Croke, B.; Jakeman, A. Addressing ten questions about conceptual rainfall–runoff models with global sensitivity analyses in R. *J. Hydrol.* **2013**, *503*, 135–152.

50. Perkins, S. E.; Pitman, A. J.; Holbrook, N. J.; McAneney, J. Evaluation of the AR4 climate models' simulated daily maximum temperature, minimum temperature, and precipitation over Australia using probability density functions. *J. Clim.* **2007**, *20*, 4356–4376.

51. Sun, Y.; Solomon, S.; Dai, A.; Portmann, R. W. How often does it rain? *J. Clim.* **2006**, *19*, 916–934.

52. Lenderink, G.; Buishand, A.; van Deursen, W. Estimates of future discharges of the river Rhine using two scenario methodologies: direct versus delta approach. *Hydrol. Earth Syst. Sci.* **2007**, *11*, 1145–1159.

53. Apata, T.; Samuel, K.; Adeola, A. Analysis of climate change perception and adaptation among arable food crop farmers in South Western Nigeria. *Contrib. Pap. Prep. Present. Int. Assoc. Agric. Econ. 2009 Conf. Beijing, China, August 16-22,2009* **2009**.

54. Tschakert, P.; Sagoe, R.; Samuel, G. O.; Codjoe, N. Floods in the Sahel : an analysis of anomalies , memory , and anticipatory learning. *Clim. Change* **2010**, *103*, 471–502.